

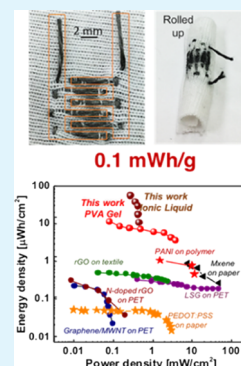
High Energy Density, Super-Deformable, Garment-Integrated Microsupercapacitors for Powering Wearable Electronics

Lushuai Zhang, Wesley Viola, and Trisha L. Andrew*¹

Departments of Chemistry and Chemical Engineering, University of Massachusetts Amherst, Amherst, Massachusetts 01003, United States

ABSTRACT: Lightweight energy storage technologies are integral for powering emerging wearable health monitors and smart garments. In-plane, interdigitated microsupercapacitors (MSCs) hold the greatest promise to be integrated into wearable electronics because of their miniaturized footprint, as compared to conventional, multilayered supercapacitors and batteries. Constructing MSCs directly on textiles, while retaining the fabric's pliability and tactile quality, will provide uniquely wearable energy storage systems. However, relative to plastic-backed or paper-based MSCs, garment-integrated MSCs are underreported. The challenge lies in creating electrochemically active fiber electrodes that can be turned into MSCs. We report a facile vapor deposition and sewing sequence to create rugged textile MSCs. Conductive threads are vapor-coated with a stably p-doped conducting polymer film and then sewn onto a stretchy textile to form three-dimensional, compactly aligned electrodes with the electrode dimensions defined by the knit structure of the textile backing. The resulting solid-state device has an especially high areal capacitance and energy density of 80 mF/cm² and 11 μW h/cm² with a polymer gel electrolyte, and an energy density of 34 μW h/cm² with an ionic liquid electrolyte, sufficient to power contemporary iterations of wearable biosensors. These textile MSCs are also super deformable, displaying unchanging electrochemical performance after fully rolling-up the device.

KEYWORDS: microsupercapacitor, fiber, reactive vapor deposition, conducting polymer, pseudocapacitor



INTRODUCTION

Long-term, continuous healthcare monitoring will be indispensable for in-home care, and early detection of abnormal physiological conditions. Driven by modern healthcare needs, novel wearable biosensors have been widely developed.^{1–5} A common challenge for the majority of wearable electronics is the lack of a suitable, portable power supply. Known examples of low-form-factor batteries are insufficient to support long-term operations, requiring frequent recharging or replacement. An alternative solution is a wearable power supply system that couples energy storage and energy harvesting circuits, which can continuously harvest ambient energy, such as solar and biomechanical energy and subsequently store it.^{6–8}

Supercapacitors are ideal candidates for wearable charge storage circuits because they have inherently higher power densities compared with batteries.^{6–8} Two main features are required of wearable supercapacitors: a high areal energy density and mechanical resilience. Flexible microsupercapacitors (MSCs) can, in theory, display both of these characteristics. With an in-plane interdigitated configuration, MSCs have significantly reduced thicknesses compared with the multilayered structure of conventional supercapacitors. Current research efforts have focused on graphene,^{9–16} conjugated polymer,¹⁷ MXene,^{18,19} or multiwalled carbon nanotubes²⁰ on flexible polymer film substrates, as well as paper-based MSCs.^{21–23} Improving upon these designs, high-performance textile-based MSCs that maintain the familiar look, feel and pliability of common textiles will be an ideal approach to wearable energy storage systems. However, incorporating

electrochemically active materials with high electrical conductivities and facilitated ionic dynamics into textiles is challenging. In recent work, nickel and reduced graphene oxide were sequentially deposited on prepatterned textiles to realize textile MSCs;²⁴ however, currently, higher energy densities are still required for practical use.

We previously reported that p-doped poly(3,4-ethylenedioxythiophene) (PEDOT-CI) coatings created using reactive vapor deposition (RVD) display high electrical conductivities on textiles^{25,26} and uniquely fatigue-resistant electrochemical characteristics.²⁷ These fundamental properties provide new opportunities for realizing high-performance textile-based MSCs using conjugated polymers.

Here, we report a high-energy density MSC sewn on a stretchy textile backing using PEDOT-CI-coated conductive threads. Thick, conformal coatings of PEDOT-CI are created over each of the microfibrils within a two-ply stainless steel thread using RVD, leading to conductive threads with high capacitance per unit length. The sewn thread arrays form three-dimensional (3D), compactly aligned electrodes with the electrode dimensions precisely defined by the knit structure of the textile backing. The resulting solid-state MSC has a high areal capacitance and energy density of 80 mF/cm² and 11 μW h/cm², respectively, with a polymer gel electrolyte and an energy density of 34 μW h/cm² with an ionic liquid electrolyte,

Received: May 21, 2018

Accepted: October 8, 2018

Published: October 8, 2018

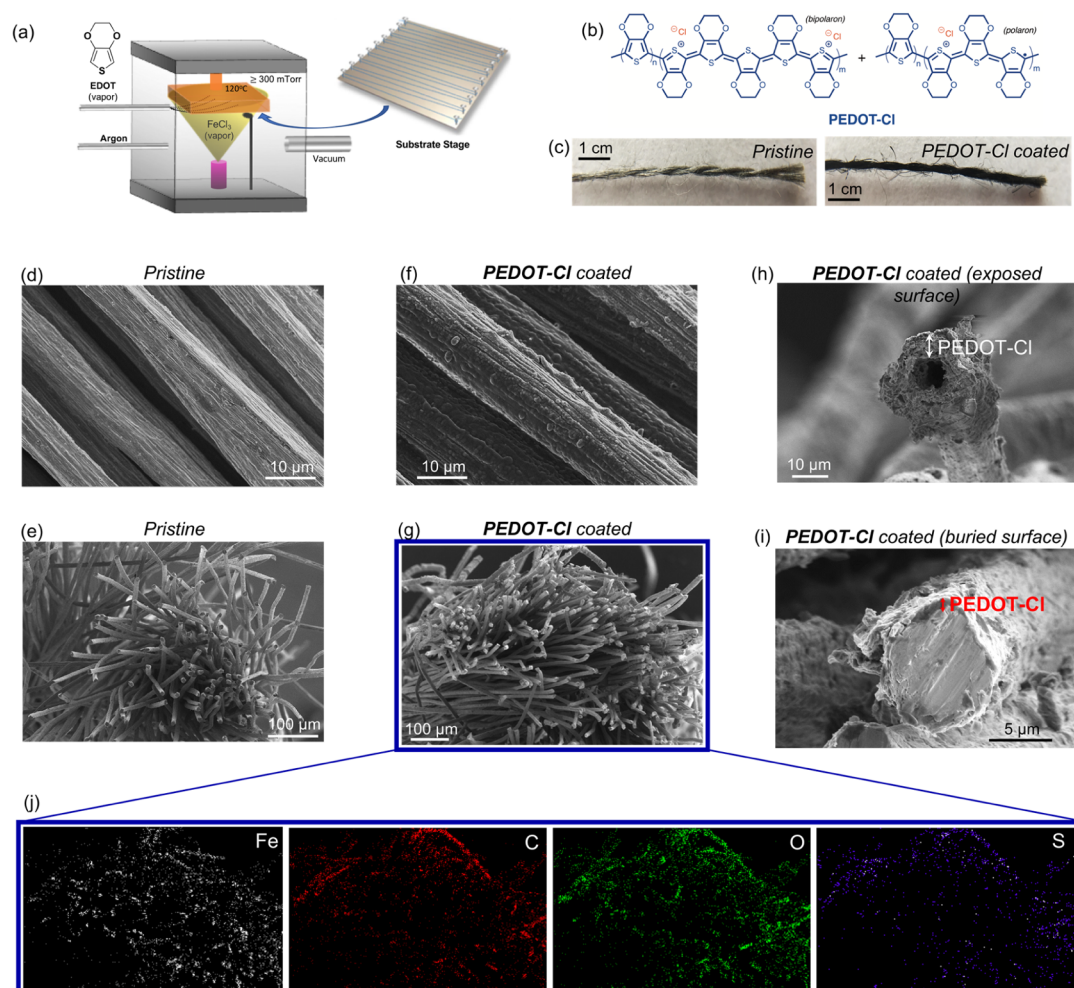


Figure 1. RVD of PEDOT-Cl and electrochemical characterization of PEDOT-Cl-coated stainless steel threads. (a) Schematic illustration of the RVD chamber. (b) Chemical structure of PEDOT-Cl created by RVD, after solvent rinsing. (c) Photographs of a pristine and PEDOT-Cl-coated stainless steel thread. (d,e) SEM images of a pristine two-ply stainless steel thread. (f,g) SEM images of a PEDOT-Cl-coated two-ply stainless steel thread. (h) SEM image of a PEDOT-Cl-coated microfibril from the surface and (i) buried core of a two-ply stainless steel thread. (j) EDX images of a PEDOT-Cl-coated stainless steel thread corresponding to the SEM image in (g).

which are 1 order of magnitude higher than those of the previously reported textile MSCs.^{24,28} These energy densities are sufficient to power selected contemporary iterations of wearable biosensors. Further, the textile MSCs reported here are also super deformable, displaying unchanging electrochemical performance after fully rolling-up the device.

MATERIALS AND METHODS

General Considerations. All chemicals were purchased from Sigma-Aldrich or TCI America and used without further purification. Field-emission scanning electron microscopy (SEM) and energy-dispersive X-ray spectroscopy (EDX) were performed using a Magellan 400.

Film Preparation. Films of p-doped PEDOT-Cl were directly deposited on stainless steel threads using a previously described reaction chamber and process parameters.^{26,27} Briefly, 3,4-ethylenedioxythiophene (EDOT) (95%, TCI America) was used as the monomer and iron(III) chloride (FeCl_3) (97%, Sigma-Aldrich) was used as the oxidant. EDOT was heated to 90 °C and was delivered into chamber through a Swagelok SS-4JB needle valve. The needle valve was open for a quarter turn. Argon gas was used to maintain the total pressure in the chamber of 300 ± 10 mTorr, and the substrate stage temperature was strictly maintained at 120 °C during deposition. Film deposition rate and the thickness were controlled

by the FeCl_3 evaporation rate, which was monitored by a quartz crystal microbalance (QCM) sensor located inside the chamber. The ratio of the actual film thickness measured post-deposition to the real-time QCM reading during deposition was recorded as the “tooling factor.” The actual film growth rate was kept at 2 nm/s. As the desired film thickness was reached, the vacuum was maintained until the substrate stage was cooled below 60 °C. The resulting films were immersed in methanol for 15 min to remove trapped iron salts and other reaction byproducts. The PEDOT-Cl films thus obtained were stably p-doped, as previously established.²⁷

Electrochemical Analysis of PEDOT-Cl-Coated Threads. PEDOT-Cl-coated stainless steel threads were characterized by three-electrode cyclic voltammetry (CV) measurements using a WaveNow potentiostat. A reference electrode of Ag/AgCl in KCl and counter electrode of platinum wire were used, and the PEDOT-Cl-coated thread served as the working electrode. Alligator clips were used to grip the PEDOT-Cl-coated threads and place them into the electrolyte solution. The electrolyte was 0.5 M aqueous Na_2SO_4 or 0.5 M aqueous H_2SO_4 .

Fabrication of Solid-State MSCs. The polymer gel electrolyte was prepared by slowly adding poly(vinyl alcohol) (PVA, 1 g) (89 000–98 000, 99%, Sigma-Aldrich) to a stirred 1 M aqueous H_2SO_4 solution (10 g). The mixture was heated at 90 °C under vigorous stirring for 2 h. Solid-state devices were prepared by casting this polymer gel electrolyte onto sewn electrodes and drying in air.

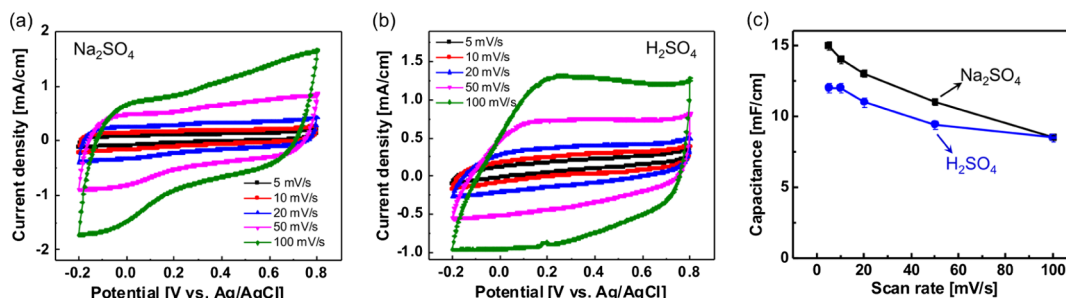


Figure 2. Cyclic voltammograms of PEDOT-Cl-coated stainless steel threads in (a) aqueous Na₂SO₄ and (b) H₂SO₄ obtained using a three-electrode setup. (c) Capacitance per unit length of PEDOT-Cl-coated stainless steel threads calculated from (a,b).

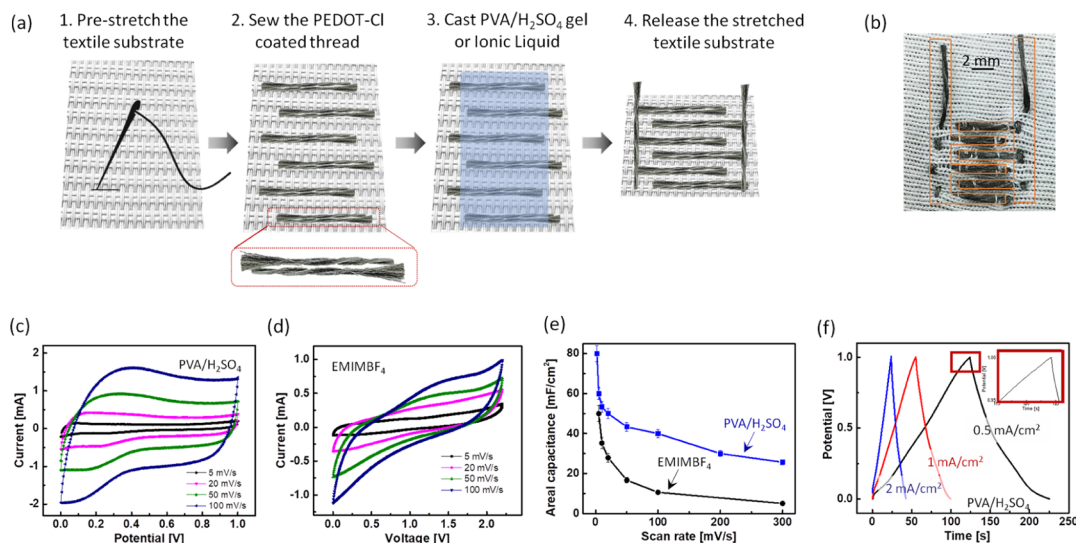


Figure 3. Fabrication and electrochemical characterization of textile MSCs. (a) Schematic illustration of the device fabrication sequence. (b) Photograph of a textile MSC with sewn electrodes (electrolyte is not shown). CV curves of textile MSCs with (c) PVA/H₂SO₄ gel electrolyte and (d) EMIMBF₄ ionic liquid electrolyte. (e) Comparison of the areal capacitances obtained from textile MSCs with different electrolytes calculated from the CV curves in (c,d). The area of the entire device is taken into consideration. (f) Galvanostatic charge/discharge curves of a textile MSC with PVA/H₂SO₄ gel electrolyte.

Alternatively, two–three drops (ca. 0.05 mL volume per drop) of ethylmethyl imidazolium tetrafluoroborate (EMIMBF₄) ionic liquid was dropped over the surface of the sewn MSC.

Electrochemical Analysis of Solid-State MSCs. Solid-state MSCs were characterized by two-electrode CV and galvanostatic charge/discharge measurements using a WaveNow potentiostat. The two separated threads of the MSC served as the two electrodes. Alligator clips were used to grip the PEDOT-Cl-coated threads from the surface of the textile MSC.

Calculations. The length-dependent capacitances of PEDOT-Cl electrodes were calculated from three-electrode CV measurements using eq 1.

$$C_{\text{electrode}} = \frac{\int j \, dV}{2\nu\Delta V} \quad [\text{F/cm}] \quad (1)$$

where j is current density normalized to the length of the PEDOT-Cl electrodes, V is voltage, ν is scan rate, and ΔV is voltage window.

The areal capacitances of solid-state PEDOT-Cl MSCs were calculated from two-electrode CV measurements using eq 2.

$$C_{\text{device}} = \frac{\int j \, dV}{2\nu\Delta V} \quad [\text{F/cm}^2] \quad (2)$$

where j is current density normalized to the entire area of the solid-state device, V is voltage, ν is scan rate, and ΔV is voltage window.

The energy densities of solid-state PEDOT-Cl MSCs were calculated using eq 3

$$E = \frac{0.5C_{\text{device}}\Delta V^2}{3600} \quad [\text{Wh/cm}^2] \quad (3)$$

where C_{device} is the areal capacitance of MSC calculated using eq 2 and ΔV is the operating voltage window of the device.

The power densities of solid-state PEDOT-Cl MSCs were calculated using eq 4

$$P = \frac{3600E\nu}{\Delta V} \quad [\text{W/cm}^2] \quad (4)$$

where E is the energy density normalized to the area of MSC including the area of the electrodes and the space between electrodes, ν is the scan rate, and ΔV is the voltage window.

RESULTS AND DISCUSSION

Figure 1 shows the schematic illustration of the RVD chamber and the substrate holder designed to uniformly coat every exposed surface of fiber/yarn substrates with persistently p-doped PEDOT-Cl.²⁶ The substrate holder allows up to 32 feet of fibers/yarns to be coated in a single deposition run.²⁶ One of the key factors for maximizing the capacitance and energy density is a high mass loading of the electrochemically active material. In solution-processed devices, the mass loading is often impeded by poor adhesion of the electronic material (which causes thick films to flake off) or limited pathways for ion transport within thick films of unoptimized morphology.

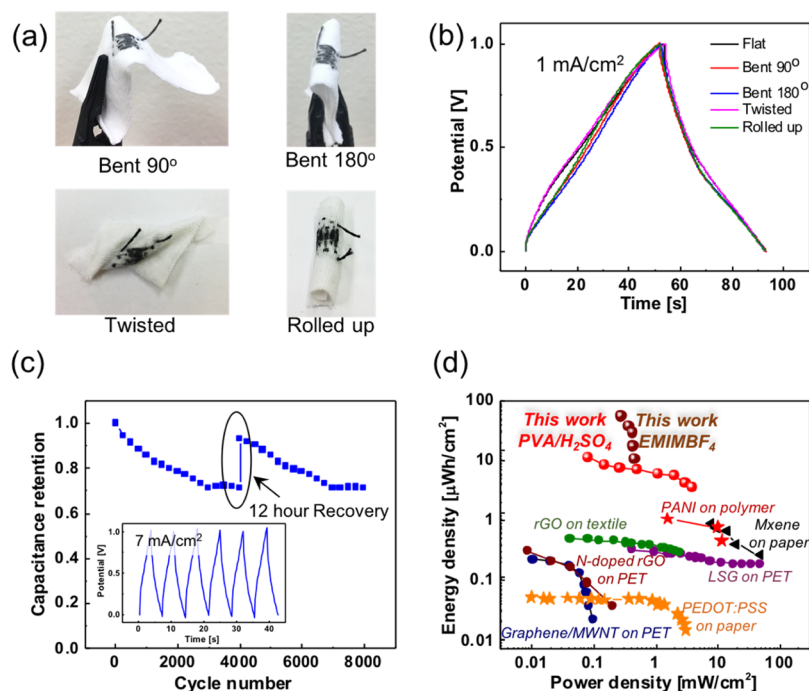


Figure 4. (a) Pictures of the textile MSC subjected to various mechanical distortions. (b) Galvanostatic charge/discharge curves measured as the device was bent, twisted, or rolled up. The charge/discharge curves of the deformed device resemble that of a flat device. (c) Cycle stability of the textile MSC measured at a fast scan rate of 7 mA/cm^2 . (d) Areal Ragone plot comparing the textile MSC reported here to other state-of-the-art flexible MSCs, including textile-based rGO MSC,²⁴ paper-based MXene²² or PEDOT:PSS²⁹ MSCs, polymer thin film-based LSG,^{30,31} PANI,³² or N-doped rGO.³³

Here, a high mass loading is achieved by depositing PEDOT-Cl on stainless steel threads via RVD. The mechanical ruggedness of vapor-deposited PEDOT-Cl coatings on various off-the-shelf textiles has been previously described.²³ Moreover, the high surface area of the stainless steel threads allows increased contact with ions from the electrolyte.

Figure 1c shows the magnified (4 \times) optical images of a pristine and PEDOT-Cl-coated two-ply stainless steel thread. Non-line-of-sight deposition leads to uniform coating of PEDOT-Cl around the thread, which maximizes the mass loading of the electroactive material. Figure 1d–g displays the cross sections of microfibril bundles without and with PEDOT-Cl coating. The two images resemble each other at this length-scale, confirming the conformal coating on each microfibril without bridging polymer films formed in between, which contributes to the mechanical ruggedness of the coating. The SEM images in Figure 1g and EDX images in Figure 1j further reveal the efficiency of the deposition on such a rough surface with an extremely high surface area. The EDX images reveal that the coating is not limited to the surface. Instead, PEDOT-Cl films are also deposited on the microfibril surfaces that are buried inside the stainless steel thread. Iron is a major component of stainless steel, whereas C, O, and S elements are contributed by PEDOT-Cl. Figure 1h,i shows the cross section of a PEDOT-Cl-coated microfibril exposed at the surface of the thread and a microfibril buried deep in the core region. The coating is $5 \mu\text{m}$ thick at the surface and $1 \mu\text{m}$ thick in the core region.

Figure 2 shows cyclic voltammograms measured with a three-electrode setup in aqueous $0.5 \text{ M Na}_2\text{SO}_4$ or $0.5 \text{ M H}_2\text{SO}_4$ using a 1 cm -long PEDOT-Cl thread as the working electrode (platinum wire counter, Ag/AgCl reference). The near rectangular voltammograms are maintained up to 100

mV/s in both electrolytes. PEDOT-Cl-coated thread capacitances per unit length at different scan rates are summarized in Figure 2c. Capacitances of 15 and 12 mF/cm are achieved at a scan rate of 5 mV/s in Na_2SO_4 and H_2SO_4 , respectively. The scan rate has a relatively mild effect on the length capacitance. At a fast scan rate of 100 mV/s , an appreciably high length capacitance of 8.5 mF/cm is retained in both electrolytes.

Figure 3 illustrates the process to create textile MSCs. Minimizing the spacing between electrode fingers is critical to obtaining a miniaturized device with reduced ion conduction lengths and maximized charge storage capabilities. The difficulty in reducing this interspace comes from the fuzziness of threads. As shown in the magnified photograph in Figure 1c, microfibrils of the stainless steel thread randomly stick out and tend to contact with microfibrils of a neighboring electrode, causing a short circuit. To address this issue, a stretchable textile is used as the substrate. For the sewing process, the substrate textile is prestretched and six interdigitated electrode fingers are alternatively sewn. We take advantage of the dimensions of the knit structure of the backing textile to confine the electrodes: the length of each electrode finger and the interelectrode spacing of the sewn MSCs are simply set by the length and width of the knit pattern of the stretchy textile backing. The neighboring electrodes are separated by two threads of the substrate textile. Each electrode is composed of two PEDOT-Cl-coated stainless steel threads stacked to form a 3D architecture, with a length of 5 mm , width of 0.6 mm , and height of 1.2 mm , presumably leading to significantly increased areal capacitance. A PVA/ H_2SO_4 gel electrolyte is then dropcast to cover all electrodes. The gel electrolyte also serves as an insulating cladding to prevent contact between electrodes. Before the electrolyte completely solidifies, the prestretched substrate is released such that the PVA gel

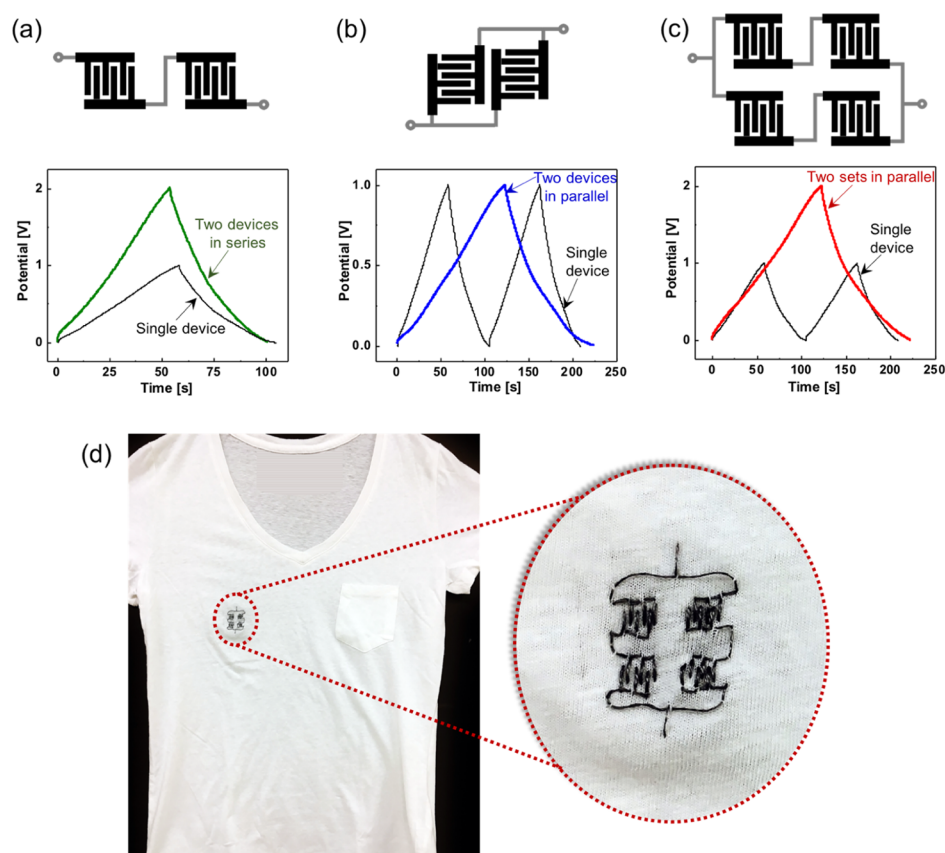


Figure 5. Galvanostatic charge/discharge curves at a current density of 1 mA/cm^2 for (a) two MSCs in a series connection, (b) two MSCs in a parallel connection, and (c) four MSCs in series and parallel connections. The galvanostatic charge/discharge curves of a single device are shown for comparison. (d) Picture of four MSCs sewn on a commercial cotton jersey T-shirt.

wrinkles (thus preventing folding-induced microcracks) and a compact, pliable device is formed. An ionic liquid electrolyte, 1-ethyl-3-methylimidazolium tetrafluoroborate (EMIMBF_4), is also explored as an alternative approach. The positive and negative electrodes are then connected by buslines. The photograph in Figure 3b shows an MSC (without gel electrolyte) after the textile is released. The overall size of a device is 6 mm in length, 5 mm in width, and 1.2 mm in height.

Figure 3c,d shows cyclic voltammograms of the textile MSC with the PVA/ H_2SO_4 gel electrolyte and EMIMBF_4 electrolyte. Areal capacitances at different scan rates are summarized in Figure 3e, where the entire device area is taken into consideration. With the PVA/ H_2SO_4 gel electrolyte, the areal capacitance is 80 mF/cm^2 at a scan rate of 2 mV/s , 60 mF/cm^2 at a scan rate of 5 mV/s , and maintained at 26 mF/cm^2 when the scan rate is increased to 300 mV/s . With EMIMBF_4 , an areal capacitance of 50 mF/cm^2 at a scan rate of 5 mV/s can be obtained. Figure 3f displays the galvanostatic charge/discharge curves of a textile MSC with the PVA/ H_2SO_4 gel electrolyte, which shows the characteristic triangle shape arising from the pseudocapacitive behavior of PEDOT-CI supercapacitors. The inset shows the enlarged graph revealing a negligible voltage drop, indicating low internal resistance within the device.

Figure 4 displays the device resilience to harsh mechanical distortions. The galvanostatic charge/discharge measurements are conducted while the device is bent at either 90° or 180° , twisted or fully rolled up. The charge/discharge traces are exactly similar to the traces obtained for a flat device. Such

high tolerance to extreme mechanical distortions is particularly important for wearable charge storage technologies, which are subjected to constant movements and deformations.

The electrochemical fatigue resistance of the solid-state textile MSC with PVA/ H_2SO_4 gel electrolyte is tested at a high rate of 7 mA/cm^2 and shown in Figure 4c. The capacitance of the device is surprisingly and reproducibly recoverable: after the first 4000 cycles, 71% of the initial capacitance is retained, which is recovered to 93% after a 12 h no-operation period. After another 4000 cycles, the capacitance again shows a 71% capacitance retention, which can be recovered to 93% after another 12 h rest period. This recoverable behavior is confirmed by multiple measurements on 12 different devices (the measurement for each device was repeated three times). One possible reason for this behavior is the redistribution of unbalanced charges in the solid-state device during the 12 h rest period.

Figure 4d compares the performance of selected, state-of-the-art flexible MSCs to those of the textile MSCs reported here. The energy density metric is particularly important for wearable MSCs. The devices reported here have energy densities of more than 1 order of magnitude higher than those of previously reported textile MSCs,²⁴ as well as those of paper^{22,29} or plastic substrate-based MSCs.^{10,30–33} Normalized to the weight of the entire device (including the textile backing, PEDOT-CI-coated thread electrodes and ionic liquid electrolyte), the textile MSC produces an energy density of 0.1 mWh/g per individual device (scan rate 5 mV/s).

Ideally, individual MSCs with optimized performance need to be connected in series or in parallel to tailor the voltage and current output required for varied, practical applications. To reduce energy losses arising from mismatched device parameters, the individual device performance needs to be highly reproducible. Reproducibility requires coating uniformity and strict control over device parameters, such as overall device area, electrode dimensions, and electrode spacing. The performance of MSCs is sensitive to the device architecture, including the dimensions of electrodes and spacing between electrodes. Normally, lithography and/or shadow-masking are/is required to micropattern electrodes. Analogous textile-based devices at microscales are difficult to obtain by hand-sewing. We take advantage of the dimensions of the knit structure of the backing textile to confine the electrodes: the length of each electrode finger and the interelectrode spacing of the sewn MSCs are simply set by the length and width of the knit pattern of the stretchy textile backing. In this way, multiple MSCs with reproducible performance can be easily embroidered on any textile that is knit in the same pattern as the common jersey cloth used here. Figure 5 shows two MSCs connected in series to produce twice the voltage output, in parallel to yield twice the current output, and in a combination of series and parallel to afford twice the voltage and current output. All data are collected at the same scanning rate of 1 mA/cm².

CONCLUSIONS

Despite remarkable progress in creating wearable and/or garment-integrated heart rate monitors and biosensors, portable power sources that can be practically integrated with these devices are not known. In-plane, interdigitated MSCs hold the greatest promise to be integrated into wearable electronics because of their miniaturized footprint, as compared to conventional, multilayered supercapacitors, and batteries. Constructing MSCs directly on textiles, while retaining the fabric's pliability and tactile quality, will provide uniquely wearable energy storage systems. However, relative to plastic-backed or paper-based MSCs, garment-integrated MSCs are underreported. The challenge lies in creating high-capacitance fiber or textile electrodes that can be turned into MSCs.

Here, we report a facile vapor deposition and sewing sequence to create rugged textile MSCs. Conductive threads are vapor-coated with a stably p-doped conducting polymer film and then sewn onto a stretchy textile to form 3D, compactly aligned electrodes with the electrode dimensions defined by the knit structure of the textile backing. The resulting solid-state device has an especially high areal capacitance and energy density of 80 mF/cm² and 11 μ W h/cm² with a polymer gel electrolyte and an energy density of 34 μ W h/cm² with an ionic liquid electrolyte, sufficient to power contemporary iterations of wearable biosensors. Further, series- and/or parallel-connected integrated charge storage circuits can be readily elaborated on commercial garments. The proof-of-concept MSC reported here opens a new window for the facile fabrication of lightweight, high-energy density textile-based MSCs that are highly tunable, are mechanically robust, and can be easily integrated into wearable power supply systems.

AUTHOR INFORMATION

Corresponding Author

*E-mail: tandrew@umass.edu.

ORCID

Trisha L. Andrew: 0000-0002-8193-2912

Author Contributions

The manuscript was written through contributions of all authors. All authors have given approval to the final version of the manuscript.

Funding

Support from the David and Lucille Packard Foundation is gratefully acknowledged.

Notes

The authors declare no competing financial interest.

REFERENCES

- (1) Liu, Y.; Pharr, M.; Salvatore, G. A. Lab-on-Skin: A Review of Flexible and Stretchable Electronics for Wearable Health Monitoring. *ACS Nano* **2017**, *11*, 9614–9635.
- (2) Huynh, T.-P.; Haick, H. Self-Healing, Fully Functional, and Multiparametric Flexible Sensing Platform. *Adv. Mater.* **2016**, *28*, 138–143.
- (3) Khan, Y.; Ostfeld, A. E.; Lochner, C. M.; Pierre, A.; Arias, A. C. Monitoring of Vital Signs with Flexible and Wearable Medical Devices. *Adv. Mater.* **2016**, *28*, 4373–4395.
- (4) Heo, J. S.; Eom, J.; Kim, Y.-H.; Park, S. K. Recent Progress of Textile-Based Wearable Electronics: A Comprehensive Review of Materials, Devices, and Applications. *Small* **2018**, *14*, 1703034.
- (5) Wang, T.; Yang, H.; Qi, D.; Liu, Z.; Cai, P.; Zhang, H.; Chen, X. Mechano-Based Transductive Sensing for Wearable Healthcare. *Small* **2018**, *14*, 1702933.
- (6) Li, L.; Lou, Z.; Chen, D.; Jiang, K.; Han, W.; Shen, G. Recent Advances in Flexible/Stretchable Supercapacitors for Wearable Electronics. *Small* **2018**, *0*, 1702829.
- (7) Lou, Z.; Li, L.; Wang, L.; Shen, G. Recent Progress of Self-Powered Sensing Systems for Wearable Electronics. *Small* **2017**, *13*, 1701791.
- (8) Qu, G.; Cheng, J.; Li, X.; Yuan, D.; Chen, P.; Chen, X.; Wang, B.; Peng, H. A Fiber Supercapacitor with High Energy Density Based on Hollow Graphene/Conducting Polymer Fiber Electrode. *Adv. Mater.* **2016**, *28*, 3646–3652.
- (9) Peng, Z.; Lin, J.; Ye, R.; Samuel, E. L. G.; Tour, J. M. Flexible and Stackable Laser-Induced Graphene Supercapacitors. *ACS Appl. Mater. Interfaces* **2015**, *7*, 3414–3419.
- (10) Peng, Z.; Ye, R.; Mann, J. A.; Zakhidov, D.; Li, Y.; Smalley, P. R.; Lin, J.; Tour, J. M. Flexible Boron-Doped Laser-Induced Graphene Microsupercapacitors. *ACS Nano* **2015**, *9*, 5868–5875.
- (11) Li, J.; Deleka, S. S.; Zhang, P.; Yang, S.; Lohe, M. R.; Zhuang, X.; Feng, X.; Östling, M. Scalable Fabrication and Integration of Graphene Microsupercapacitors Through Full Inkjet Printing. *ACS Nano* **2017**, *11*, 8249–8256.
- (12) Li, L.; Secor, E. B.; Chen, K.-S.; Zhu, J.; Liu, X.; Gao, T. Z.; Seo, J.-W. T.; Zhao, Y.; Hersam, M. C. High-Performance Solid-State Supercapacitors and Microsupercapacitors Derived from Printable Graphene Inks. *Adv. Energy Mater.* **2016**, *6*, 1600909.
- (13) Liu, Z.; Wu, Z.-S.; Yang, S.; Dong, R.; Feng, X.; Müllen, K. Ultraflexible In-Plane Micro-Supercapacitors by Direct Printing of Solution-Processable Electrochemically Exfoliated Graphene. *Adv. Mater.* **2016**, *28*, 2217–2222.
- (14) Wang, S.; Wu, Z.-S.; Zheng, S.; Zhou, F.; Sun, C.; Cheng, H.-M.; Bao, X. Scalable Fabrication of Photochemically Reduced Graphene-Based Monolithic Micro-Supercapacitors with Superior Energy and Power Densities. *ACS Nano* **2017**, *11*, 4283–4291.
- (15) Xiao, H.; Wu, Z.-S.; Chen, L.; Zhou, F.; Zheng, S.; Ren, W.; Cheng, H.-M.; Bao, X. One-Step Device Fabrication of Phosphorene

and Graphene Interdigital Micro-Supercapacitors with High Energy Density. *ACS Nano* **2017**, *11*, 7284–7292.

(16) Zhang, L.; DeArmond, D.; Alvarez, N. T.; Malik, R.; Oslin, N.; McConnell, C.; Adusei, P. K.; Hsieh, Y.-Y.; Shanov, V. Flexible Micro-Supercapacitor Based on Graphene with 3D Structure. *Small* **2017**, *13*, 1603114.

(17) Wu, Z.-S.; Zheng, Y.; Zheng, S.; Wang, S.; Sun, C.; Parvez, K.; Ikeda, T.; Bao, X.; Müllen, K.; Feng, X. Stacked-Layer Heterostructure Films of 2D Thiophene Nanosheets and Graphene for High-Rate All-Solid-State Pseudocapacitors with Enhanced Volumetric Capacitance. *Adv. Mater.* **2017**, *29*, 1602960.

(18) Peng, Y.-Y.; Akuzum, B.; Kurra, N.; Zhao, M.-Q.; Alhabeab, M.; Anasori, B.; Kumbur, E. C.; Alshareef, H. N.; Ger, M.-D.; Gogotsi, Y. All-MXene (2D titanium carbide) Solid-State Microsupercapacitors for On-Chip Energy Storage. *Energy Environ. Sci.* **2016**, *9*, 2847–2854.

(19) Li, H.; Hou, Y.; Wang, F.; Lohe, M. R.; Zhuang, X.; Niu, L.; Feng, X. Flexible All-Solid-State Supercapacitors with High Volumetric Capacitances Boosted by Solution Processable MXene and Electrochemically Exfoliated Graphene. *Adv. Energy Mater.* **2017**, *7*, 1601847.

(20) Kim, S.-K.; Koo, H.-J.; Lee, A.; Braun, P. V. Selective Wetting-Induced Micro-Electrode Patterning for Flexible Micro-Supercapacitors. *Adv. Mater.* **2014**, *26*, 5108–5112.

(21) Guo, R.; Chen, J.; Yang, B.; Liu, L.; Su, L.; Shen, B.; Yan, X. In-Plane Micro-Supercapacitors for an Integrated Device on One Piece of Paper. *Adv. Funct. Mater.* **2017**, *27*, 1702394.

(22) Kurra, N.; Ahmed, B.; Gogotsi, Y.; Alshareef, H. N. MXene-on-Paper Coplanar Microsupercapacitors. *Adv. Energy Mater.* **2016**, *6*, 1601372.

(23) Li, R.-Z.; Peng, R.; Kihm, K. D.; Bai, S.; Bridges, D.; Tumuluri, U.; Wu, Z.; Zhang, T.; Compagnini, G.; Feng, Z.; Hu, A. High-Rate In-Plane Micro-Supercapacitors Scribed onto Photo Paper Using in Situ Femtolaser-Reduced Graphene Oxide/Au Nanoparticle Micro-electrodes. *Energy Environ. Sci.* **2016**, *9*, 1458–1467.

(24) Pu, X.; Liu, M.; Li, L.; Han, S.; Li, X.; Jiang, C.; Du, C.; Luo, J.; Hu, W.; Wang, Z. L. Wearable Textile-Based In-Plane Micro-supercapacitors. *Adv. Energy Mater.* **2016**, *6*, 1601254.

(25) Zhang, L.; Fairbanks, M.; Andrew, T. L. Rugged Textile Electrodes for Wearable Devices Obtained by Vapor Coating Off-the-Shelf Plain-Woven Fabrics. *Adv. Funct. Mater.* **2017**, *27*, 1700415.

(26) Zhang, L.; Baima, M.; Andrew, T. L. Transforming Commercial Textiles and Threads into Sewable and Weavable Electric Heaters. *ACS Appl. Mater. Interfaces* **2017**, *9*, 32299–32307.

(27) Zhang, L.; Andrew, T. L. Deposition Dependent Ion Transport in Doped Conjugated Polymer Films: Insights for Creating High-Performance Electrochemical Devices. *Adv. Mater. Interfaces* **2017**, *4*, 1700873.

(28) Jost, K.; Dion, G.; Gogotsi, Y. Textile Energy Storage in Perspective. *J. Mater. Chem. A* **2014**, *2*, 10776–10787.

(29) Liu, W.; Lu, C.; Li, H.; Tay, R. Y.; Sun, L.; Wang, X.; Chow, W. L.; Wang, X.; Tay, B. K.; Chen, Z.; Yan, J.; Feng, K.; Lui, G.; Tjandra, R.; Rasenthiram, L.; Chiu, G.; Yu, A. Paper-Based All-Solid-State Flexible Micro-Supercapacitors with Ultra-High Rate and Rapid Frequency Response Capabilities. *J. Mater. Chem. A* **2016**, *4*, 3754–3764.

(30) El-Kady, M. F.; Kaner, R. B. Scalable Fabrication of High-Power Graphene Micro-Supercapacitors for Flexible and On-Chip Energy Storage. *Nat. Commun.* **2013**, *4*, 1475.

(31) Yun, J.; Kim, D.; Lee, G.; Ha, J. S. All-solid-state Flexible Micro-Supercapacitor Arrays with Patterned Graphene/MWNT Electrodes. *Carbon* **2014**, *79*, 156–164.

(32) Meng, C.; Maeng, J.; John, S. W. M.; Irazoqui, P. P. Ultrasmall Integrated 3D Micro-Supercapacitors Solve Energy Storage for Miniature Devices. *Adv. Energy Mater.* **2014**, *4*, 1301269.

(33) Liu, S.; Xie, J.; Li, H.; Wang, Y.; Yang, H. Y.; Zhu, T.; Zhang, S.; Cao, G.; Zhao, X. Nitrogen-Doped Reduced Graphene Oxide for High-Performance Flexible All-Solid-State Micro-Supercapacitors. *J. Mater. Chem. A* **2014**, *2*, 18125–18131.